Identification of positively charged carbon antisite-vacancy pairs in 4*H*-SiC

T. Umeda and J. Ishoya
Graduate School of Library, Information, and Media Studies, University of Tsukuba, Tsukuba 305-8550, Japan

T. Ohshima, N. Morishita, and H. Itoh
Japan Atomic Energy Agency, Takasaki 370-1292, Japan

A. Gali
Department of Atomic Physics, Budapest University of Technology and Economics, Budafoki út 8, H-1111 Budapest, Hungary
(Received 24 January 2007; revised manuscript received 18 April 2007; published 7 June 2007)

An antisite-vacancy pair and a monovacancy are a set of fundamental stable and/or metastable defects in compound semiconductors. Theory predicted that carbon antisite-vacancy pairs would be much more stable in *p*-type SiC than silicon vacancies and that they would be a common defect. However, no experimental evidence has yet supported this prediction. We reexamine electron-irradiated *p*-type 4*H*-SiC and identify the positively charged carbon antisite-vacancy pairs ($C_{Si}V_C^+$) by means of electron paramagnetic resonance and *ab initio* calculations. We compare them with other coexisting defects such as carbon vacancy (V_C) and divacancy ($V_{Si}V_C$) and show that $C_{Si}V_C$ and V_C are very similar in terms of thermal stability and electronic levels.

DOI: 10.1103/PhysRevB.75.245202 PACS number(s): 61.72.Ji, 71.55.Ht, 71.15.Mb, 76.30.Mi

I. INTRODUCTION

In the past decade, silicon carbide (SiC) single crystals have been intensively studied for the development of a novel wide-gap semiconductor electronics. As-grown, irradiated, and heat-treated crystals show a variety of lattice defects related to silicon and carbon atoms. In 4*H*-SiC, which is the most studied SiC single crystal, combined studies of electron paramagnetic resonance (EPR) spectroscopy and first-principles calculation have identified four types of fundamental defects. These have been observed in many samples. The first type of defect is a silicon vacancy (V_{Si}), which can be thermally stable in the *n*-type region.[1,2] This vacancy can be observed in the form of the −1 charge state in *n*-type[3] and semi-insulating (SI) SiC.[4] There coexist two distinguishable types of such vacancies: the V_{Si}^- (I)/(II) center [nearly undistorted V_{Si}^- at *k*/*h* sites, *S* (electron spin) =3/2 (Refs. 5 and 6)] and the T_{V2a} center [V_{Si}^- with *c*-axial distortion, $S=3/2$ (Ref. 3)]. The second type of defect is a carbon vacancy (V_C) that exhibits the opposite behavior; namely, it becomes increasingly stable in the *p*-type region.[1,2] Therefore, the +1 charge state (V_C^+) is often observed in *p*-type[7] and SI materials[4,8] (*EI*5 and *EI*6 center at *k* and *h* sites,[7] respectively, $S=1/2$), while in some *n*-type[9] or SI SiC (Ref. 4) the −1 charge state (V_C^-) is also detectable (the *HEI*1 or *SI*6 center,[9,10] $S=1/2$). The third type of defect is a divacancy[11,12] ($V_{Si}V_C$) that can be observed in the form of neutral states (the *P*6 and *P*7 centers, on- and off-axis pairs of $V_{Si}V_C^0$, respectively, $S=1$).[12] The divacancy signal appeared strongly in SI (Refs. 12 and 13) or *n*-type SiC,[12,14] which is consistent with the theory[11] that it is energetically favored in the *n*-type region. The fourth type of defect is a carbon antisite-vacancy (AV) pair.[14] This pair is a stable and/or metastable counterpart of V_{Si}.[2,15] Recently, this type was identified in *n*-type and SI SiC (the *SI*5 center, $C_{Si}V_C^-$, $S=1/2$).[14]

Theoretically, all four types can be highly thermally stable in SiC.[1,2,11,15,16] However, theory predicted that, alone among them, the carbon AV pair is much more stable in the positive charge state in the *p*-type region.[2,15] Therefore, positively charged carbon AV pairs should be easily detected in *p*-type or SI SiC. Although many studies have been done on these types of SiC, no experimental evidence has yet supported the presence of the AV defects. Their single positive charge state ($C_{Si}V_C^+$) can have an electron spin of 1/2 and should be detectable by EPR.

If the $C_{Si}V_C^+$ pairs were as stable as predicted by theory, it could be important in *p*-type and SI SiC and could be correlated with important defects. For example, deep-level transient spectroscopy revealed famous thermally stable defects of $Z_{1/2}$ (E_V+2.6 eV) and $EH_{6/7}$ (E_V+1.7 eV) in 4*H*-SiC.[17] A recent study[18] suggested that both of these types of defect are related to either a V_C-related defect or a single V_C. In this model, the $Z_{1/2}$ and $EH_{6/7}$ levels were correlated with negative and positive charge states of the defects, respectively. If the negative and positive charge states of $C_{Si}V_C$ were both thermally stable, they might also be candidates for such important defects.

We carefully reexamined electron-irradiated *p*-type 4*H*-SiC and identified the *missing* $C_{Si}V_C^+$ pairs by means of EPR measurements and *ab initio* supercell calculations. Our results clearly indicate that the $C_{Si}V_C$ defect can be an abundant and important defect in *p*-type SiC, supporting the predictions of earlier theoretical studies.[2,15] We also estimated thermal stability and electronic levels of $C_{Si}V_C$ by comparing them with other coexisting defects such as V_C and $V_{Si}V_C$. We found that the $C_{Si}V_C$ and V_C defects are quite similar; both defects exhibit a similar thermal stability and similar positive and negative electronic levels.

II. EXPERIMENT

To create $C_{Si}V_C^+$ defects, we carried out 3 MeV electron irradiation of commercial boron-doped *p*-type 4*H*-SiC substrates (room-temperature carrier concentration=10^{15} cm^{-3})

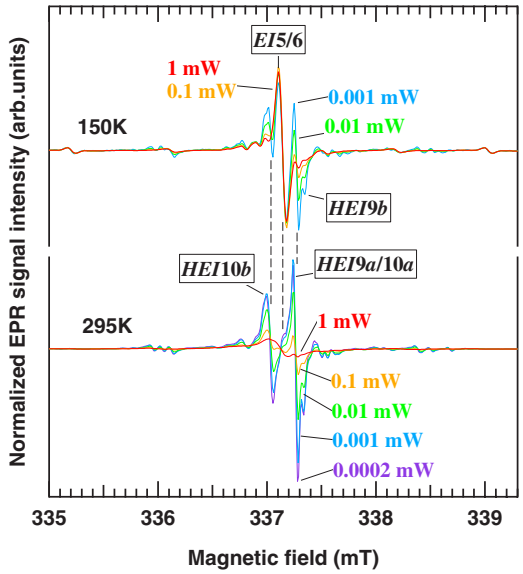

FIG. 1. (Color online) Microwave saturation effect of EPR centers in electron-irradiated *p*-type 4*H*-SiC measured at 150 and 295 K. EPR spectra were normalized by a factor of (microwave power)$^{1/2}$. In these spectra, well-known *EI*5/6 signals (overlapped) and four EPR signals (*HEI*9*a*/9*b*/10*a*/10*b*) were detected. Latter signals exhibit a much stronger saturation effect than former signals.

at temperatures from 800 to 850 °C. With the same irradiation of *n*-type 4*H*-SiC, we obtained a high concentration of $C_{Si}V_C$ defects ($C_{Si}V_C^-$).[14] Therefore, we expected a similar situation in the *p*-type samples. To obtain a sufficient signal-to-noise ratio, we used 1.5-mm-thick substrates and enhanced the defect concentration by high electron doses of 2×10^{18}, 4×10^{18}, and 10×10^{18} e/cm^2. After the irradiation, the samples became virtually semi-insulating. This had the advantage of minimizing a dielectric loss of microwaves due to free carriers in a substrate.

The EPR spectra were measured in the dark (thermal equilibrium) by a Bruker Bio-Spin E500 X-band spectrometer with a high-*Q*-factor (>10 000) microwave cavity. Microwave frequency was set to 9.452 GHz, and EPR signals were detected by a 100 kHz magnetic-field modulation with 0.05 mT amplitude. Most of the measurements were carried out at room temperature (295 K), while an Oxford ESR900 liquid-He cryostat system was used for low-temperature measurements.

There is a simple reason why the $C_{Si}V_C^+$ EPR centers have not yet been observed. Figure 1 shows a series of 150 and 295 K EPR spectra measured at different microwave powers. In both temperatures, when the microwave power was reduced, instead of the well-known *EI*5/6 EPR signal from positively charged carbon vacancies (V_C^+),[7] other EPR signals became clear. We named them *HEI*9*a*/*b* and *HEI*10*a*/*b*.[19] As the temperature decreased from 295 to 150 K, the microwave saturation effect worked more dramatically for the *HEI*9/10 signals. Eventually, these signals became negligibly small at the lower temperatures (for example, 4–80 K) used in previous studies.[4,7–9,12–14] Therefore, we studied the *HEI*9/10 EPR centers at room temperature and at the lowest microwave power (0.2 μW). Because these conditions greatly reduced EPR signal intensities, we had to use the signal-enhancement techniques noted above.

In Fig. 2, the four EPR signals were measured without the saturation effect. Each signal originates from an electron spin of 1/2. Their angular dependences, which are plotted in Fig. 3(a), reveal a C_{3v} symmetry for the two *HEI*9 centers and C_{1h} symmetry for the two *HEI*10 centers. Their *g* tensors show similar principal values but their symmetric axes ($g_\parallel$ axes), which are summarized in Table I, are different. By analogy with the *P*6/*P*7 EPR centers in 4*H*-SiC (neutral divacancies, $V_{Si}V_C^0$),[12] we assume that the *HEI*9/10 centers belong to the same defect but have different orientations of $C_{Si}V_C$. Namely, the C_{3v} centers (*HEI*9) may correspond to on-axis $C_{Si}V_C$ pairs (parallel to the *c* axis), while the C_{1h} centers (*HEI*10) may be off-axis pairs (parallel to a basal Si-C bond). In addition to this variation, the 4*H*-SiC crystal has two inequivalent lattice sites, called the cubic (*k*) and hexagonal (*h*) sites. In total, there are four different configurations and/or EPR signals for $C_{Si}V_C$.

The identification of the $C_{Si}V_C$ pairs is based on ^{13}C hyperfine (HF) interactions caused by their C_{Si} atoms. The magnified (×10 and ×20) spectra in Fig. 2 reveal very weak HF doublets created by ^{13}C (nuclear spin $I=1/2$, natural abundance=1.1%). The signal intensity ratios of each HF

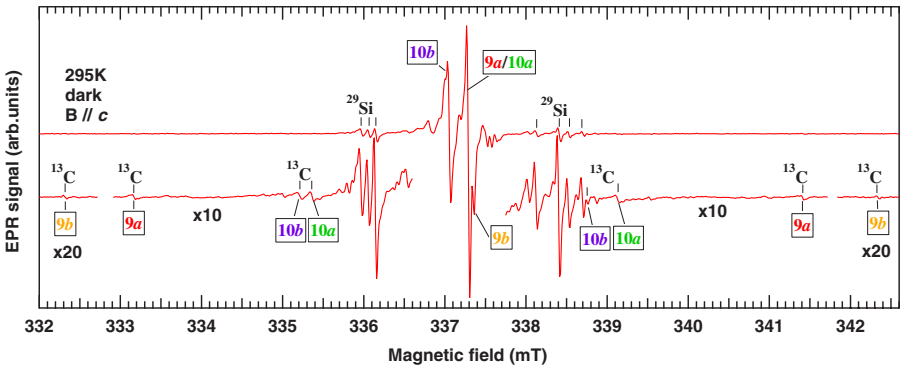

FIG. 2. (Color online) EPR spectra of *p*-type 4*H*-SiC after 1×10^{19} e/cm^2 irradiation measured at 295 K using a microwave power of 0.2 μW. At this power, *HEI*9/10 EPR signals (depicted by 9*a*, 9*b*, 10*a*, and 10*b*, respectively) were observed without microwave saturation effect.

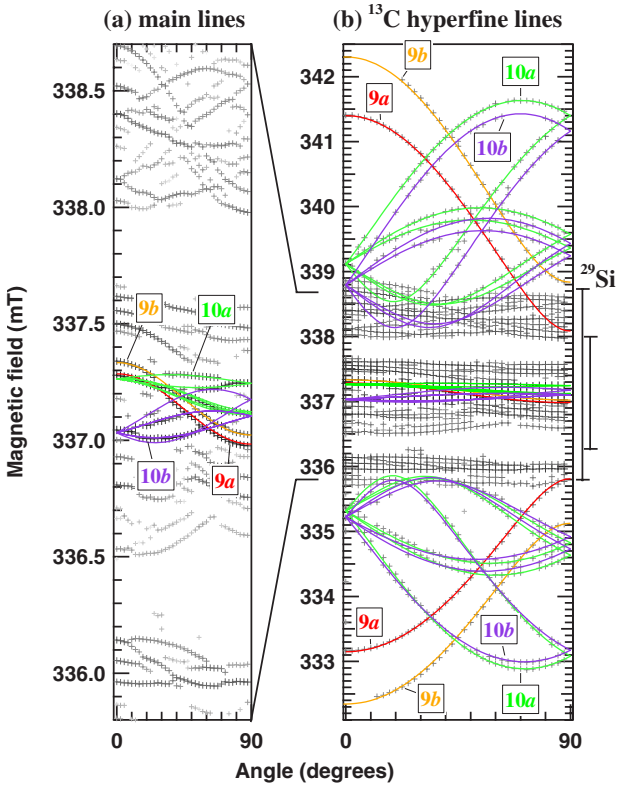

FIG. 3. (Color online) Angular maps for *HEI*9/10 centers. Magnetic field was rotated from [0001] (0°) to [$\bar{1}$100] (90°). Solid lines are simulated results using spin-Hamiltonian parameters shown in Table I.

doublet to each main line are 5.3/480 (1.1%) for *HEI*9*a*, 2.5/158 (1.6%) for *HEI*9*b*, 8.9/1020 (0.9%) for *HEI*10*a*, and 7.4/781 (0.9%) for *HEI*10*b*, where we separated the overlapped main lines of *HEI*9*a* and *HEI*10*a* using a different spectrum, which was measured for a 90° angle. These ratios indicate that every *HEI*9/10 center is localized mainly on a single carbon atom. The next largest HF interactions are caused by ^{29}Si (I=1/2, natural abundance=4.7%), which generates a number of much stronger HF satellites (see Fig. 2) with splitting widths between 1.7 and 2.9 mT [see Fig. 3(b)]. Unfortunately, due to the complicated overlapping, it was difficult to accurately analyze them. Therefore, we focused on the ^{13}C HF interactions.

The angular dependences of the observed ^{13}C HF interactions could be excellently fitted, as shown in Fig. 3(b), using the spin-Hamiltonian parameters (the g and HF tensors) in Table I. The ^{13}C HF tensors are axially symmetric, so they can be well described by contributions of carbon 2s and 2p orbitals. By comparing the standard HF constants for ^{13}C (A_{2s}=134.77 mT, A_{2p}=3.83 mT),[20] we estimated the carbon 2s and 2p orbital fractions in each defect wave function to be 3% and 52% for *HEI*9*a*, 4% and 54% for *HEI*9*b*, 4% and 53% for *HEI*10*a*, and 3% and 53% for *HEI*10*b*. The wave functions are quite similar in each signal, just forming carbon dangling bonds (DBs). The DB directions (the θ angles of the ^{13}C HF tensors) are parallel to the c axis for *HEI*9*a*/*b* (θ=0°) and parallel to a basal bond for *HEI*10*a*/*b* (θ=109°). These carbon DBs can be reasonably attributed to the C_{Si} atoms of on-axis/off-axis carbon AV pairs shown in Figs. 4(a) and 4(b), respectively. Since the samples were of p type and the observed electron spin was 1/2, it is reasonable to assign a single positive charge state ($C_{Si}V_C^+$) to the relevant centers. More complete identification of $C_{Si}V_C^+$ is given by means of *ab inito* supercell calculations described below, where we can distinguish the four configurations of $C_{Si}V_C$ [(*hh*), (*kk*), (*hk*), and (*kh*); see Fig. 4] from the four EPR centers.

III. THEORETICAL IDENTIFICATION

Ab initio calculations based on density-functional theory in the local-density approximation[21] with the Ceperley-Alder

TABLE I. Spin-Hamiltonian parameters of four *HEI*9/10 centers and four $C_{Si}V_C^+$ pairs in 4*H*-SiC. Spin Hamiltonian is expressed as $H=\mu_B\mathbf{S}\cdot\mathbf{g}\cdot\mathbf{B}+\Sigma_i\,\mathbf{S}\cdot\mathbf{A}(i)\cdot\mathbf{I}(i)-g_N\mu_N\mathbf{I}(i)\cdot\mathbf{B}$ as defined in Ref. 9, where $\mathbf{g}$ is a g tensor and $\mathbf{A}(i)$ is a hyperfine (HF) tensor for a nuclear spin i. θ expresses angle between main ($\|$) principal axis and c axis. Measured and calculated HF constants are expressed in mT. Associated Si atoms found by theory are defined in Fig. 4. For (*kh*) and (*hk*) configurations, three additional detectable ^{29}Si HF interaction lines were found near C_{Si}, which is not labeled here or in Fig. 4.

		g				**A** ($^{13}C_{Si}$)				**A** (^{29}Si)
Center	Symmetry	g_{xx}	g_{yy}	g_{zz} ($g_\|$)	θ	A_{xx}	A_{yy}	A_{zz} ($A_\|$)	θ	$A_{xx,yy,zz}$
EPR measured at 295 K										
*HEI*9*a*	C_{3v}	2.00408	2.00408	2.00227	0°	2.27	2.27	8.25	0°	1.7–2.9
*HEI*9*b*	C_{3v}	2.00379	2.00379	2.00195	0°	3.71	3.71	9.95	0°	1.7–2.9
*HEI*10*a*	C_{1h}	2.00348	2.00258	2.00226	145°	2.60	2.65	8.75	109°	1.7–2.9
*HEI*10*b*	C_{1h}	2.00399	2.00345	2.00263	116°	2.31	2.45	8.44	109°	1.7–2.9
Theory for $C_{Si}V_C^+$ in 4*H*-SiC										
(*hh*)	C_{3v}					1.96	1.96	7.01	0°	2.1–2.9 (Si_{4-6})
(*kk*)	C_{3v}					3.12	3.12	8.59	0°	2.1–2.9 (Si_{4-6})
(*kh*)	C_{1h}					1.69	1.70	6.14	110°	2.5–3.4 (Si_1)
(*hk*)	C_{1h}					1.65	1.67	6.00	108°	2.1–2.7 ($Si_{2,3}$)

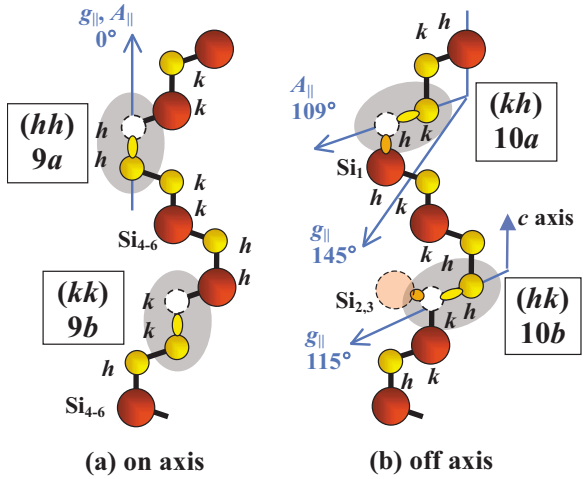

FIG. 4. (Color online) Atomic models for four $C_{Si}V_C$ pairs in 4*H*-SiC. This figure shows a lattice structure in $(11\bar{2}0)$ plane of crystal. Four *HEI*9/10 centers correspond to four configurations of $C_{Si}V_C^+$. Angles between *c* axis and main (‖) principal axes of *g* and HF tensors are noted. Carbon (silicon) atoms are drawn as small (large) balls, and their dangling bonds are drawn as small ovals. Open balls are carbon vacancies.

exchange correlation[22] were carried out in the framework of the SIESTA (Ref. 23) and CPPAW codes.[24] A 256-atom hexagonal supercell of 4*H*-SiC was used with 2^3 Monkhorst-Pack *K*-point set[25] to model the defects. First, the geometry was optimized by SIESTA code (see Ref. 26 for details), then the geometry was reoptimized, and, finally, the HF tensor was calculated by the all-electron CPPAW code (see Ref. 7 for details). All four possible configurations were considered in our study. The on-axis (*hh*) and (*kk*) configurations have C_{3v} symmetry, while the (*hk*) and (*kh*) configurations have C_{1h} symmetry. In the optimized structures, the on-axis configurations will produce one a_1 defect level at about E_V (valence-band edge) +1.3 eV and a double-degenerate *e* level in the upper part of the band gap, while the off-axis configurations with lower symmetry have one a' level at about E_V +1.2 eV and two close levels (a' and a'') in the upper part of the band gap. As was explained for the on-axis configurations in our previous study,[14] the deep a_1 defect level is mostly localized on the carbon antisite (C_{Si}) while the *e* level is localized on the carbon vacancy part of the complex. In $C_{Si}V_C^+$, the a_1 level of (*hh*)/(*kk*) configurations [and the lower a' level of (*hk*)/(*kh*) configurations] is occupied by one electron, while the *e* level (or a' and a'' levels) are empty.

The on-axis configurations have an a_1 character, conserving the C_{3v} symmetry after geometry optimization, which is consistent with the experimental results. In the relaxed structures, there is a subtle difference between the geometry of the (*hh*) and (*kk*) configurations: in the (*hh*) configuration, the C_{Si} atom is relaxed more strongly backward than in the (*kk*) configuration. This results in weaker ^{13}C HF interaction in (*hh*) than in (*kk*) configuration, which can account for the observed difference between *HEI*9*a*/*b*. In fact, the calculated HF tensors are in good agreement with those of *HEI*9*a*/*b* taking the possible error in the local-density approximation (LDA) functional and the supercell size into account (Table I). Therefore, we identify *HEI*9*a* as the (*hh*) configuration and *HEI*9*b* as the (*kk*) one, as shown in Fig. 4(a). The localization of the spin density in the carbon vacancy is negligible in this case. Because of the strong localization of the spin density on the C_{Si} atom, the localization of the spin density is detectable on the second-neighbor Si atoms of the C_{Si} atom along the *c* axis, depicted as Si_{4-6} in Fig. 4(a).

For the off-axis configurations, ^{13}C HF interactions were only slightly different between the *HEI*10*a*/*b* centers or the calculated (*kh*) and (*hk*) configurations (Table I). However, the two a' levels can be slightly mixed in the off-axis configurations. As a result, the spin density also distributes on either the Si_1 or $Si_{2,3}$ atoms of V_C, as illustrated in Fig. 4(b). The calculations also predict that three second-neighbor Si atoms of the C_{Si} atom have HF constants similar to those of Si_{1-3}. A total of four or five ^{29}Si HF interactions will be measurable, which can account for a number of the observed ^{29}Si HF lines in Fig. 2. For the (*kh*) center, we speculate that the spin density on Si_1 can turn the $g_{\|}$ principal axis toward the direction of the Si_1 atom. Therefore, we assign *HEI*10*a* (θ=145° for $g_{\|}$) to the (*kh*) configuration and *HEI*10*b* (θ =115°) to the (*hk*) configuration. For these cases, the agreement between the calculated and measured HF tensors of C_{Si} atom is not as good as for the on-axis case, but we still believe it to be reasonable. We think that the orbital mixing of the C_{Si} atom and the silicon DBs may cause larger error in the LDA calculation than in the on-axis configurations, where this orbital mixing is absent.

When the Fermi level E_F is positioned above E_V+1.2 ~1.3 eV as the a_1 or a' level of $C_{Si}V_C$ being singly occupied, the divacancy may be negatively charged and also cause a spin-1/2 EPR center. Note that its (0|–) level was predicted to be about E_V+1.4 eV.[12] We have also checked this possibility. The HF parameters of a negatively charged divacancy were already calculated by Gerstmann *et al.*[16] They reported that, as with $C_{Si}V_C^+$, $V_{Si}V_C^-$ (in 3*C*-SiC) generates the single largest ^{13}C HF interaction. However, the calculated ^{13}C HF constants of $A_{\|(zz)}$=155 MHz (5.53 mT) and $A_{\perp(xx,yy)}$=63 MHz (2.24 mT) do not fit our experimental values (see Table I). In particular, the 2*p* orbital density [=$(A_{\|}-A_{\perp})/3/A_{2p}$] (Ref. 20) on the main ^{13}C atom is estimated to be only 29% for $V_{Si}V_C^-$ as against 52%–54% (38%–48%) in our experiments (calculation). Therefore, we can exclude the $V_{Si}V_C^-$ model as an explanation of the origin of *HEI*9/10.

IV. THERMAL STABILITY AND ELECTRONIC LEVEL OF CARBON AV PAIRS

First, we compared the thermal stability of the carbon AV pairs with that of other coexisting defects in irradiated SiC. In thermal equilibrium, all irradiated *p*-type samples showed dominant EPR signals of $C_{Si}V_C^+$ (*HEI*9/10) and V_C^+ (*EI*5/6). As is plotted in Fig. 5(a), their concentrations were quite comparable; e.g., after 4×10^{18} e/cm^2 irradiation, 3.2×10^{17} and 2.5×10^{17} cm^{-3} for $C_{Si}V_C^+$ and V_C^+, respectively. This implies that the formation energy or kinetics is similar

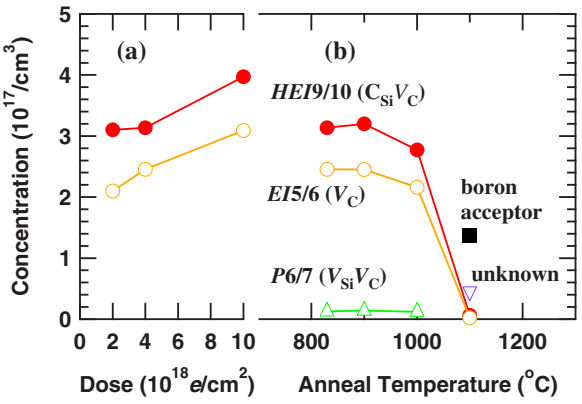

FIG. 5. (Color online) Concentrations of *HEI*9/10 centers and other coexisting defects in electron-irradiated *p*-type 4*H*-SiC: (a) electron irradiation performed at around 800 °C, and (b) a sample after 4×10^{18} e/cm^2 irradiation was subjected to isochronal annealing. *HEI*9/10 ($C_{Si}V_C^+$), *EI*5/6 (V_C^+), and unknown signals were observed at room temperature, whereas neutral boron acceptor (B_k^0) and *P*6/7 ($V_{Si}V_C^0$) signals were measured at 30 K. Concentrations were estimated in thermal equilibrium (in dark), except for *P*6/7 center where its concentration was nominally estimated under 100 W halogen lamp illumination.

for both defects. The $V_{Si}V_C^0$ (*P*6/*P*7) signal, on the other hand, was absent in thermal equilibrium but weakly observed under illumination at low temperatures (nominally 0.1×10^{17} cm^{-3}).

Next, an irradiated sample (electron dose=4×10^{18} e/cm^2) was subjected to isochronal annealing in Ar ambient for 30 min. The result is shown in Fig. 5(b). The $C_{Si}V_C^+$ and V_C^+ defects exhibited a very similar behavior; they were almost unchanged after 1000 °C annealing, but 95% of them were annealed out at 1100 °C. The $V_{Si}V_C^0$ signal also disappeared at this stage. We simultaneously observed the recovery of boron acceptors and the generation of weak unknown signals. Note that the above annealed-out temperature for $C_{Si}V_C$, V_C, and $V_{Si}V_C$ was lower than that observed for other types of samples (1200–1500 °C).[4,12–14,17] This can be ascribed to a different E_F position and different abundances of defects among the samples. In any case, we infer that $C_{Si}V_C^+$ pairs have a thermal stability comparable to that of V_C^+ or $V_{Si}V_C^0$.

The finding that $C_{Si}V_C^+$ and V_C^+ coexisted but $V_{Si}V_C^0$ did not appear in thermal equilibrium means that electronic levels of $C_{Si}V_C^+$ and V_C^+ are located close to each other, and at this energy position, $V_{Si}V_C$ defects should not be neutral. We speculate that $V_{Si}V_C$ defects are most probably negatively charged, as discussed earlier, and tentatively speculate that the E_F position higher than $E_V+1.4$ eV is required for this case.[12] On the other hand, for V_C, two photoinduced EPR data were reported for *p*- and *n*-type 4*H*-SiC.[9,27] In both types, a rapid increase in the *EI*5 EPR signal (V_C^+) was detected with approximately 1.8 eV optical excitation. This increase was caused by the conversion of V_C^- or V_C^0 into V_C^+, which was in turn caused by excitation of electron(s) from V_C to the conduction band.[9,27] Therefore, V_C^+ defect levels must be generated in $E_C-1.8$ eV ($E_V+1.5$ eV) and lower. On the basis of these considerations, we speculate that $C_{Si}V_C^+$ defect levels are distributed at around $E_V+1.4\sim1.5$ eV, which is a range similar to that for V_C^+. This speculation does not conflict with the calculated a_1 or a' levels for $C_{Si}V_C^+$ ($E_V+1.2\sim1.3$ eV).

V. SUMMARY

We have identified the *missing* positively charged carbon AV pairs ($C_{Si}V_C^+$) in electron-irradiated *p*-type 4*H*-SiC by means of EPR and *ab initio* supercell calculation. Theory predicted that such pairs should be thermally stable in the *p*-type region.[2,14,15] The reason they have not been observed in previous studies was simply that a strong microwave saturation effect hindered their EPR signals under optimum conditions for conventional EPR experiments. We have found four EPR centers, *HEI*9*a*/*b* ($S=1/2$, C_{3v} symmetry) and *HEI*10*a*/*b* ($S=1/2$, C_{1h} symmetry), which have been successfully assigned to $C_{Si}V_C^+(hh)/(kk)$ and $C_{Si}V_C^+(kh)/(hk)$, respectively, on the basis of EPR and theoretical analyses of their ^{13}C hyperfine interactions. Their wave functions were strongly localized on each C_{Si} atom, originating from the a_1 or a' character of their paramagnetic electronic levels (calculated at about $E_V+1.2\sim1.3$ eV). An isochronal annealing study suggested that the thermal stability of $C_{Si}V_C^+$ is as high as that of V_C^+. It was also suggested that electronic levels of both $C_{Si}V_C^+$ and V_C^+ are located at around $E_V+1.4\sim1.5$ eV, whereas $V_{Si}V_C$ should not be neutral in this range. Furthermore, in previous works,[9,14] electronic levels of $C_{Si}V_C^-$ and V_C^- were found in the same range of $E_C-1.1$ eV and deeper. On the whole, the $C_{Si}V_C$ defects are quite similar to the V_C defects, meaning they can coexist in SiC.

ACKNOWLEDGMENT

Support of Grant No. NIIF-1090 from the National Information Infrastructure Development Program in Hungary is appreciated.

[1] A. Zywietz, J. Furthmüller, and F. Bechstedt, Phys. Rev. B **59**, 15166 (1999).
[2] M. Bockstedte, A. Mattausch, and O. Pankratov, Phys. Rev. B **68**, 205201 (2003).
[3] N. Mizuochi, S. Yamasaki, H. Takizawa, N. Morishita, T. Ohshima, H. Itoh, T. Umeda, and J. Isoya, Phys. Rev. B **72**, 235208 (2005).
[4] N. T. Son, B. Magnusson, Z. Zolnai, A. Ellison, and E. Janzén, Mater. Sci. Forum **457–460**, 437 (2004).
[5] N. Mizuochi, S. Yamasaki, H. Takizawa, N. Morishita, T. Ohshima, H. Itoh, and J. Isoya, Phys. Rev. B **68**, 165206 (2003).
[6] M. Bockstedte, M. Heid, and O. Pankratov, Phys. Rev. B **67**,

193102 (2003).
[7] T. Umeda, J. Isoya, N. Morishita, T. Ohshima, T. Kamiya, A. Gali, P. Deák, N. T. Son, and E. Janzén, Phys. Rev. B **70**, 235212 (2004).
[8] M. E. Zvanut, W. Lee, H. Wang, W. C. Mitchel, and W. D. Mitchel, Mater. Sci. Forum **527–529**, 517 (2006).
[9] T. Umeda, Y. Ishitsuka, J. Isoya, N. T. Son, E. Janzén, N. Morishita, T. Ohshima, H. Itoh, and A. Gali, Phys. Rev. B **71**, 193202 (2005).
[10] We suggest that the *SI*6 (SI-6) center in high purity SI 4*H*-SiC samples (Ref. 4) is identical to the *HEI*1 center (Ref. 9) by judging from their *g* factor along the *c* axis as well as photoinduced EPR data in Refs. 4 and 9.
[11] L. Torpo, T. E. M. Staab, and R. M. Nieminen, Phys. Rev. B **65**, 085202 (2002).
[12] N. T. Son, P. Carlsson, J. ul Hassan, E. Janzén, T. Umeda, J. Isoya, A. Gali, M. Bockstedte, N. Morishita, T. Ohshima, and H. Itoh, Phys. Rev. Lett. **96**, 055501 (2006).
[13] W. E. Carlos, N. Y. Garces, E. R. Glaser, and M. A. Fanton, Phys. Rev. B **74**, 235201 (2006).
[14] T. Umeda, N. T. Son, J. Isoya, E. Janzén, T. Ohshima, N. Morishita, H. Itoh, A. Gali, and M. Bockstedte, Phys. Rev. Lett. **96**, 145501 (2006).
[15] E. Rauls, T. Frauenheim, A. Gali, and P. Deák, Phys. Rev. B **68**, 155208 (2003).
[16] U. Gerstmann, E. Rauls, and H. Overhof, Phys. Rev. B **70**, 201204(R) (2004).
[17] Y. Negoro, T. Kimoto, and H. Matsunami, Appl. Phys. Lett. **85**, 1716 (2004), and references therein.
[18] K. Danno and T. Kimoto, J. Appl. Phys. **100**, 113728 (2006).
[19] These centers were preliminary reported as *HEI*9/10/11 in T. Umeda, N. Morishita, T. Ohshima, H. Itoh, and J. Isoya, Mater. Sci. Forum **556–557**, 453 (2007). Here we would like to rename them as *HEI*9/10 according to our complete identification of $C_{Si}V_C^+$ described in this paper.
[20] J. A. Weil, J. R. Bolton, and J. E. Wertz, in *Electron Paramagnetic Resonance* (Wiley, New York, 1994).
[21] W. Kohn and L. J. Sham, Phys. Rev. Lett. **140**, A1133 (1965).
[22] D. M. Ceperley and B. J. Alder, Phys. Rev. Lett. **45**, 566 (1980).
[23] D. Sanchéz-Portal, P. Ordejón, E. Artacho, and J. M. Soler, Int. J. Quantum Chem. **65**, 543 (1997).
[24] P. E. Blöchl, C. J. Först, and J. Schimpl, Bull. Mater. Sci. **26**, s33 (2001).
[25] H. J. Monkhorst and J. K. Pack, Phys. Rev. B **13**, 5188 (1976).
[26] A. Gali, P. Deák, P. Ordejon, N. T. Son, E. Janzén, and W. J. Choyke, Phys. Rev. B **68**, 125201 (2003).
[27] N. T. Son, B. Magnusson, and E. Janzén, Appl. Phys. Lett. **81**, 3945 (2002).